Research Square

Preprints are preliminary reports that have not undergone peer review.
They should not be considered conclusive, used to inform clinical practice,
or referenced by the media as validated information.

Nervous system mediated cardiac arrest in mangrove killifish

Tetsuhiro Kudoh

t.kudoh@exeter.ac.uk

University of Exeter https://orcid.org/0000-0002-5373-2737

Rosalie Herbert

University of Exeter

Alexander Corbett

University of Exeter https://orcid.org/0000-0003-1645-5475

Article

Keywords: Mangrove killifish, heartbeat, diapause, HSPD

Posted Date: October 29th, 2026

DOI: https://doi.org/10.21203/rs.3.rs-11429892/v1

License: This work is licensed under a Creative Commons Attribution 4.0 International License. Read Full License

Additional Declarations: There is **NO** Competing Interest.

Abstract

Generating and regulating the heartbeat in response to both internal physiological cues and the external environment is mediated by conserved autonomic neural pathways. Heart rate regulation is fundamental to survival, and while it is dynamic, complete cessation is often associated with pathology or extreme physiological stress. However, we have found an abrupt and complete heart-stopping behavior that occurs frequently, causes no harm, and is followed by full recovery. Here we show that embryos of the mangrove killifish, *Kryptolebias marmoratus*, exhibit heart-stopping in response to physical disturbance (HSPD). Tactile or vibrational stimulation triggers embryos to stop their hearts, sometimes for over a minute, before restarting and beating normally. This behavior begins in the later stages of embryonic development prior to hatching and is retained throughout diapause. We show that HSPD is a developmentally regulated, neuronally mediated and plastic response, shaped by sensory input. These findings identify a previously undescribed form of cardiac regulation involving neural and intrinsic cardiac system interactions. This work provides new insight into how sensory stimulation influences vertebrate cardiac activity and contributes to establishing *K. marmoratus* as a model for studying conserved neurocardiac mechanisms relevant to cardiac rhythm regulation and dysfunction.

Summary/introduction

Heartbeat regulation is fundamental to vertebrate survival, enabling continuous response to both internal physiological demands and the external environment. Cardiac rhythm is generated by intrinsic pacemaker cells, continuously modulated by the autonomic nervous system (ANS)[1–3]. The ANS comprises two branches, the sympathetic and parasympathetic nervous systems (SNS and PSNS), which exert opposing effects on heart rate, conduction velocity and contractility to maintain stability and meet physiological demands[4–9]. The cardiac ANS consists of neural networks both outside the heart, and within the heart itself – the intracardiac nervous system, where innervation is both extensive and diverse[4,10]. Together, these form a distributed network enabling continuous, rapid and flexible modulation of cardiac activity. Disruption of these pathways contributes to arrhythmias, heart failure and sudden cardiac death[9,11], highlighting the importance of understanding how they develop and interact.

Cardiac activity is influenced not only by internal physiology but also environmental sensory inputs. A well-described example is the conserved vertebrate startle response, a rapid defensive reaction to stimulation, accompanied by autonomic modulation of cardiac activity[12–15]. In teleosts such as zebrafish, the response emerges during embryonic development, with behavioural outputs increasing and becoming region-dependent as sensory neurons differentiate[15,16]. Associated with these behaviours are conserved biphasic cardiac responses: an initial parasympathetically mediated bradycardia followed by delayed sympathetic tachycardia[7,17–20].

Reponses to stimulation are often adaptive and plastic. Habituation, the progressive reduction in responsiveness to repeated stimulation, can occur, reflecting reduced neurotransmitter release[21]. This is observed in zebrafish with repeated vibrational stimuli[17], also rats and humans[14,19,20]. In contrast, sensitisation involves increased responsiveness, associated with increased neurotransmitter release.

Sensitisation has also been reported across teleosts and mammals[22–24]. However, the mechanisms by which stimulus type, frequency, and intensity influence whether habituation or sensitisation occurs is unclear[21]. Likewise, the relationship between sensory circuit maturation, development of extrinsic and intrinsic cardiac regulatory systems, and the relative contributions of each autonomic branch is poorly understood[17,25]. To address these questions, a suitable vertebrate model with quantifiable interactions between sensory input and cardiac regulation is required.

The mangrove killifish, *Kryptolebias marmoratus*, is an emerging vertebrate model that is exceptionally tolerant of harsh and variable environmental conditions. Individuals can tolerate emersion and widely ranging salinities and temperatures[26–28], and embryos can enter diapause, a state of arrested development, when conditions are unfavourable[29,30]. Being optically transparent and chemically manipulable[31], *K. marmoratus* are an excellent model for investigating physiological adaptations for stress tolerance and plasticity.

Intentional heart stopping by animals is an exceptionally rare phenomenon. Stopping or significantly reducing the heart rate is also known to occur in some animals when in a state of dormancy such as hibernation or diapause[32,33]. However, an abrupt and complete heart-stopping behavior that occurs frequently, causes no harm, and is followed by full recovery, has not previously been reported.

Here, we report a previously undescribed behaviour in *K. marmoratus* embryos, termed heart stopping in response to subtle physical disturbance (HSPD), in which subtle tactile or vibrational stimulation induces a transient cardiac arrest which is followed by fast and full recovery. We characterise the developmental emergence of HSPD, investigate the contributions of neural and intrinsic cardiac regulatory mechanisms, examine how different sensory stimuli influence the response, and explore its potential adaptive significance.

Unlike the bradycardia associated with the vertebrate startle response, HSPD involves complete cessation of beating, with heart stops sometimes lasting over a minute before full recovery. HSPD is first observed during late embryonic development prior to hatching and is retained during diapause. Whether HSPD is an extreme version of conserved startle-induced bradycardia or a distinct phenomenon is unknown.

During diapause, embryos survive outside the water, exposed to small predators that may sense vibrations from their heart beating. Suspending beating when nearby movement is detected could therefore reduce detectability. Therefore, the HSPD could act as an anti-predation strategy.

By providing a live, quantifiable readout of interactions between sensory input, autonomic regulation and intrinsic cardiac systems *in vivo*, HSPD offers a unique system to investigate vertebrate cardiac regulation. Beyond revealing a previously undescribed behavior, this work has broader biomedical relevance establishing *K. marmoratus* as a promising model for studying how autonomic branches interact to maintain cardiac stability, with potential relevance to understanding arrhythmias and developing therapeutic strategies[34,35].

Results

Developmental progression of HSPD

The heart of the *K. marmoratus* embryos started beating at 3 days post fertilization (dpf), as previously reported[31]. At the later stage of embryonic development from 9dpf, a peculiar heart stopping in response to physical disturbance (HSPD) was observed. The physical disturbances that triggered HSPD included gentle touching of the chorion (Supp. video 1) or by tapping the petri dish containing the embryos (Fig. 1). At 9dpf, stops were short, with full recovery averaging 8 seconds. From 9dpf to 14dpf, the duration of heart stops and the recovery time increased from 8 seconds to 75 seconds (Fig. 2, supp. Figure 1).

Around 13dpf, embryonic development is complete, and embryos can either hatch or enter diapause[31]. Most embryos in our experiments entered diapause, delaying hatching. The HSPD ability was retained during diapause. However, once embryos entered diapause (~ 14dpf), lengths of heart stops and recovery periods became more variable (Supp. Figure 1). While embryos were responsive to physical stimuli, light stimulation (light on/off) did not induce HSPD (data not shown). During HSPD, the heartbeat ceased, but other movements, including those of the eyes, mouth and gills did not stop. This indicated that HSPD does not cause complete paralysis of the body (Supp. video 2). Embryos were highly sensitive, as gently touching the chorion with the tip of a tweezer induced HSPD and stops could exceed 60 seconds (exemplified in supp. video 1).

Baseline pre-stimulus heart rates increased throughout development, peaking at 82 bpm at 11dpf, before declining to 67 bmp at 13dpf. Heart rates remained reduced throughout the diapause period, albeit with high variability (Supp. Figure 2). Diapause heart rates were significantly lower than at both 11 and 12dpf (mean differences 12.38 and 10.71bpm, $p = 0.0022$ and 0.0082, $z = 3.0512$ and 2.6427, respectively).

Heart stopping and restarting occurs in the sinus venosus

In *K. marmoratus* embryos, individual contractions of the sinus venosus, atrium and ventricle were clearly distinguishable and could be measured independently (Fig. 3). Stimulation caused the heart to stop immediately, the last beat always ending with the ventricle contracting (Fig. 3E). During HSPD, the sinus venosus and atrium remained filled with blood, as in diastole, and passive flow into the ventricle was often observed. The first beat after HSPD consistently began with contraction of the sinus venosus (Fig. 3F). These results indicate that the order of chamber contractions is always sinus venosus, atrium, ventricle.

The time between each chamber contracting remained regular even during the recovery period after HSPD (Fig. 3). There was no significant difference in the timing between contractions of individual chambers before and after HSPD ($p > 0.25$). Before HSPD, the average time after contraction of the sinus venosus for atrial and ventricular contractions were 0.23s and 0.62s, respectively. After HSPD, these were 0.25s and 0.65s. Together, these suggest the heart stop is always initiated by the sinus venosus.

Pharmacological modulation of HSPD

To examine molecular and physiological mechanisms of HSPD, various chemical inhibitors that may affect heart rate regulation were applied. Firstly, tubocurarine, a neuromuscular blocker, did not affect HSPD though average heart rate was reduced suggesting that response to the physical stimulus by skeletal muscle is not involved in the HSPD. In contrast, general anesthetics, phenoxyethanol or tricaine, completely abolished HSPD indicating the involvement of neuronal circuitry being involved in the HSPD. To further narrow down specific neuronal regulatory mechanisms, neurotransmitter inhibitors for sympathetic and parasympathetic neurons, propranolol and atropine, were tested respectively. As a result, atropine abolished HSPD suggesting a crucial role of parasympathetic nervous system in HSPD. Propranolol did not suppress HSPD but reduced the duration of HSPD suggesting a supportive role of sympathetic neuron in maintaining HSPD. Other neurotransmitter inhibitors, dizocilpine, gabazine and ketanserin, which inhibit glutamatergic, GABAergic and serotonergic signaling, were also tested showing reduced duration of HSPD. These results suggest the crucial role of parasympathetic neurons on triggering HSPD and supportive role of several nervous systems in modifying the duration of the HSPD.

Compared to control, baseline HR was significantly reduced by 2-phenoxyethanol, tubocurarine and propranolol ($p < 0.015$) (Supp. Figure 3, Table 1). All drugs except tubocurarine significantly affected HR_{50} ($p < 0.0004$): propranolol, dizocilpine, gabazine and ketanserin reduced HR_{50}; 2-phenoxyethanol, tricaine and atropine completely inhibited HSPD, reducing HR_{50} to zero (Fig. 4, Table 1).

HSPD is shaped by sensory integration and habituation

Stimulus strength

To test if the response of HSPD depends on the level of physical stimulation, quantitatively reproducible levels of stimulation were given to embryos using the pendulum-based mechanical stimulation setup (Fig. 1). The data showed that for all embryonic stages tested (10 to 14dpf), the length of heart stops was stimulus-dependent, with stronger stimuli inducing longer heart stops (Fig. 5A).

Multiple successive stimuli

The effect of multiple successive stimuli varied in developmental stages (Fig. 5B). At 10–13 dpf, increasing stimulus number increased HR_{50}, indicating cumulative integration of stimulus strength. At 14dpf (possibly at diapause) embryos showed the longest HR_{50} from the 1st and did not show a clear increase of HR_{50} suggesting the development of HSPD is fully mature and the full response may be achieved with the 1st stimulus.

Continuous stimulation

For all ages, repeated stimulation at 10-second intervals for 20 minutes caused an initial suppression of cardiac activity, followed by a gradual recovery despite continued stimulation (Fig. 6A). Within 1–2 minutes, BC10s values, defined as beat count per 10-second interval between stimulation, showed either complete cessation or large reductions from baseline (Table 2). This varied by age: 9–10 dpf embryos showed

reduced BC10s, whereas for ages 11–13 dpf, BC10s were reduced to zero. Time to reach minimum BC10s also varied by age (Table 2).

Following the initial suppression, cardiac activity resumed and BC10s increased despite ongoing stimulation. Mean BC10s at the start of stimulation, end of stimulation, and 5-minutes post stimulation were compared with baseline. As some data deviated from normality ($W = 0.73–0.83$, $p < 0.05$), non-parametric tests were used. For all ages, BC10s during the first 60 seconds of stimulation were significantly reduced from baseline ($p < 0.05$). BC10s during the final 60 seconds of stimulation increased from the first 60 seconds, but remained below baseline, but this was only statistically significant for 12–13 dpf ($p < 0.05$). Five minutes post-stimulation, BC10s returned to levels insignificantly different to baseline for all ages, indicating full recovery (Fig. 6Aii).

Linear models provided a good fit for 10–13 dpf, indicating approximately linear recovery dynamics. The 9 dpf time series showed a poorer fit, due to a non-linear response characterized by rapid early recovery followed by a plateau. Therefore, a shorter window (first 15 minutes) was modelled for 9 dpf, improving the fit (Fig. 6Ai, Table 2). Overall, recovery dynamics differed across ages where younger embryos habituated faster.

Stimulation repeated at 5-minute intervals

Across all ages, stimulation repeated at 5-minute intervals reduced both baseline HR and HR_{50}. While repeated stimulation reduced responsiveness, with HR_{50} generally decreasing across repeated stimulation, changes were variable and non-linear (Fig. 6B). These data suggest that multiple stimuli with either short or long intervals can cause desensitization.

HSPD does not occur in dechorionated embryos

To assess effects of region-specific stimulation, 12 dpf embryos were dechorionated and gently touched at different regions with a needle (Fig. 7C). However, once dechorionated, embryos no longer showed the prolonged cardiac arrests characteristic of HSPD (Fig. 7A&B). To confirm this was not due to differences in stimulation type (touching versus pendulum-based), dechorionated embryos were also assessed with the standard pendulum-based stimulation but still did not show HSPD. Data for HR data did not significantly deviate from normality ($p = 0.332$, $w = 0.912$) so parametric tests were used. Dechorionated embryos' HR were significantly lower than control ($p = 0.0005$, $tstat=-5.603$), with a means of 54.4 bpm (SD = 6.1) and 70.7 bpm (SD = 6.6), respectively.

Due to the lack of prolonged heart stops, inter-beat interval (IBI) was used instead of HR_{50} to assess responses to stimulation (Fig. 7D&E). Data did not significantly deviate from normality, so parametric tests were used. T-tests showed that the first IBI post-stimulation was significantly increased relative to baseline for all stimulation regions ($p < 0.03$, $tstat = 2.461–5.371$). This effect was transient, as subsequent IBIs did not differ significantly from baseline ($tstat=-0.876-1.568$, $p > 0.1$). Responses also varied spatially, with greater increases in IBI following stimulation at anterior regions, decreasing posteriorly. These indicate that

the dechorionated embryo can still respond to the stimuli, but HSPD does not occur. This may suggest that an alternative response is occurring, such as startle response.

Table 1
Effects of pharmacological treatments on heart rate (HR) and HR_{50} compared to control. Statistical comparisons are shown for HR and HR_{50} with the Wilcoxon rank-sum test (*p* = *p*-value, W = test statistic).

Treatment	**HR (mean ± SD)**		***p* (HR)**	**W (HR)**	**HR_{50} (mean ± SD)**		***p* (HR_{50})**	**W (HR_{50})**
Control	70.667	± 6.633	-	-	36.667	± 11.180	-	-
2-Phenoxyethanol	52.889	± 2.472	4.11×10^{-5}	126.0	0	-	4.11×10^{-5}	126.0
Tricaine	73.667	± 6.384	0.346	74.5	0	-	4.11×10^{-5}	126.0
Tubocurarine	40.667	± 5.385	4.11×10^{-5}	126.0	38.333	± 14.5774	0.74	81.5
Atropine	74.000	± 4.796	0.303	73.5	0	-	4.11×10^{-5}	126.0
Propanolol	49.556	± 18.809	0.015	112.5	3.333	± 5.000	4.11×10^{-5}	126.0
Dizocilpine	76.308	± 4.608	0.075	76.5	6.923	± 9.473	1.59×10^{-4}	159.5
Gabazine	68.000	± 6.083	0.618	91.5	9.444	± 8.819	1.23×10^{-4}	124.5
Ketanserin	70.222	± 7.775	0.783	89.0	10.000	± 10.308	4.11×10^{-4}	122.5

Table 2

Beat count response and recovery parameters during recurring 10-second stimulation in embryos aged 9–13 dpf. BC time-series data were generated from mean beat counts across 10-second intervals (BC10s) between stimulation. Absolute and relative BC10s reductions were calculated from baseline, and time to reach minimum BC10s from the onset of stimulation. Recovery from this minimum was modelled using linear regression. *For 9 dpf, the model was only fitted over the first 15 minutes of the post-minimum response period due to non-linear recovery dynamics over the full window. Goodness of fit is reported as the coefficient of determination (R^2) and root mean square error (RMSE).

Age (dpf)	Absolute BC10s drop	Relative BC10s drop (%)	Time To Min. BC10s	Recovery Slope	Intercept	R^2	RMSE
9 *	10.482	86.281	90	0.493	4.027	0.922	0.565
10	12.889	99.145	110	0.451	0.092	0.961	0.482
11	11.259	100	50	0.377	-0.520	0.903	0.690
12	13.296	100	0	0.224	-0.235	0.923	0.377
13	12.704	100	10	0.182	-0.032	0.892	0.365

Discussion

We have discovered a peculiar heart stopping behavior of mangrove killifish embryos in response to physical disturbance where the heart beating stops following tactile or vibrational stimulation. This HSPD may occur frequently in the wild, considering cause can be attributed to even very slight physical disturbance. We demonstrate that HSPD is not a simple reflex, but a plastic, neuronally mediated behavior. HSPD requires coordinated autonomic and central nervous system activity, emerges alongside cardiac innervation, and is shaped by sensory input and stimulus history, raising the possibility that it may function as an anti-predation strategy. To our knowledge, this has not been reported in any other species.

HSPD as a part of embryonic developmental process occurring before diapause/hatching

Embryos consistently acquired the HSPD ability around 9dpf, with all embryos able to stop their hearts by 10dpf. The duration of stops increased until the end of development at 13-14dpf. This indicates that the acquisition and development of the HSPD ability is part of the highly synchronized embryonic development in *K. marmoratus*, and it occurs prior to hatching/diapause.

When embryos reach 13dpf, some embryos start hatching[31]. Therefore, from 14dpf onward, embryos that did not hatch likely entered a diapause - a state of arrested development where metabolic rate is significantly reduced, used to cope with stressful conditions[30]. Supporting this, baseline heart rates reduced at 13dpf and remained low during diapause (Supp. Figure 2). The initial reduction at 13dpf may mean that some embryos have already entered diapause or are preparing for it. As metabolism is reduced during diapause, the animal must prioritize which processes or functions energy is put into. This indicates that HSPD is of high importance for survival or coping with stressors during the diapause period.

Although metabolic rate is generally low during diapause, there can be wide variation between individuals[36]. This was evident in the reduced, but highly variable baseline heart rates in diapause embryos (Supp. Figure 2). Within this time there may also be pre-diapause preparatory phases or post-diapause recovery phases, during which metabolic rates can vary[30]. Additionally, the length of diapause is highly variable, previous studies reporting lengths ranging from 23 to 108 days[37]. These factors may contribute to the observed variation in HSPD recovery time in diapause-stage embryos compared to the clear pattern seen in 9-14dpf embryos, especially if recovery is linked to metabolic rate. This suggests that the development of HSPD is complete by 14dpf, and the variable "depth" of diapause may lead to variability in the level of HSPD.

Other killifish species (*Nothobrancheus furzeri* and *Austrofundulus limnaeus*) have been reported to reduce their heart rates that occurs as metabolism is reduced during diapause, sometimes to the extent they appear to stop completely[38,39]. However, in these species the heart stops without physical stimulation, and it occurs earlier on in embryonic development. In contrast, HSPD in *K. marmoratus* is an immediate, short-lived reaction to physical stimulation. It may be possible that the mechanisms to reduce/stop the heartbeat during diapause seen in *N. furzeri* and *A. limnaeus* may be exploited in the mangrove killifish to develop the ability of HSPD.

HSPD has not been reported in other fish species, suggesting that it may be an evolutionary survival strategy unique to *K. marmoratus*. It is conceivable that HSPD may have two advantages for embryos. Firstly, as mentioned above, HSPD is possibly a function associated with diapause. By being able to control heart rate, the embryo may be able to preserve energy in diapause. The second potential advantage of HSPD may be related to predator avoidance. *K. marmoratus* often inhabits crab burrows. During dry seasons they may remain in these small spaces with limited water supplies for weeks or months within a state of diapause. This could increase risk of predation by creatures such as small crabs. HSPD may reduce vibrations or electric pulses that could be detected by hair sensors of small crabs searching for food in these burrows. This was suggested by imitating the movement of a crab's claw using the tip of a pair of tweezers and observing how this very small physical disturbance induced HSPD (Supp. video 1). Stopping the heartbeat to reduce metabolism and avoid predation may continue to be advantageous for juveniles and adults. Therefore, it would be interesting to investigate HSPD in hatched fish for future research. Alternatively, HSPD may not confer any adaptive advantages. It may be a result of linkage to other genes under selection, or the high levels of inbreeding and homozygosity in the mangrove killifish, which have arisen from selfing and may have led to the fixation of the trait[40].

The sinus venosus in HSPD initiation and recovery

We observed that contraction of chambers was always sinus venosus, atrium then ventricle. Before HSPD, the ventricle was always the last chamber to contract and after, the sinus venosus was the first. After HSPD, timings of contractions of chambers within individual heartbeats remained the same as before HSPD, despite heart rate starting slower before recovering to the original rate. Vertebrate hearts are myogenic, generating their own rhythm independent of the brain by pacemaker cells. In fish, these pacemaker cells are located in a ring-like shape at the sinus node[41]. Therefore, it seems likely that the pacemaker cells are involved in regulation of HSPD. In mammalian hearts, the atrioventricular (AV) node delays the electrical

signal from the atrium to ventricle – fish have an analogous structure within the AV junction to fulfil this role [42]. Similarly, there is a delay between the sinus venosus and atrium contracting[43]. Together, our results indicate that the key domain in which stopping and restarting occurs is the sinus venosus, and the other two chambers cannot stop or restart contraction on their own, and these delays are unaffected.

HSPD is mediated by integrated autonomic mechanisms

While results suggest that the sinus venosus is the key domain of the heart determining the initiation of HSPD and release from it, pharmacological experiments were conducted to elucidate whether regulation was entirely autonomous to the heart. Pharmacological manipulation indicates that HSPD is neuronally mediated. The general anesthetics phenoxyethanol and tricaine (MS-222) both inhibited HSPD. In contrast, blocking skeletal muscle contraction with tubocurarine did not affect HR_{50}. As general anaesthetic supresses neural activity, these confirm HSPD is dependent on neural mechanisms rather than direct myogenic or muscular activity.

Further pharmacological evidence demonstrates that HSPD requires coordinated autonomic regulation. Blocking PSNS activity with atropine inhibited HSPD. In contrast, blocking SNS activity with propranolol significantly reduced HR_{50} without completely inhibiting HSPD. Together, these indicate that PSNS activity drives heart stopping, while SNS activity modulates the magnitude and recovery. While the PSNS and SNS have opposing effects on cardiac function[44], they interact at multiple levels (e.g. intrinsic cardiac nervous system, spinal cord, brain) and can be co-activated, causing electrical instability if dysregulated[45]. Considering inhibition of either autonomic branch suppressed HSPD, these indicate that HSPD requires coordinated activity rather than activation of a single branch.

The involvement of additional neurotransmitter systems suggests multiple neural systems integrate to regulate HSPD. Antagonists of glutamatergic (dizocilpine) and GABAergic (gabazine) signaling reduced HR_{50} without inhibiting HSPD. These demonstrate that both excitatory and inhibitory pathways shape the response, either through central circuits or the intracardiac nervous system. Overall, these show that the balance of multiple neural systems is important for determining the duration of HSPD, and disruption to any of these alters the duration of response.

Further work to quantify sympathetic and parasympathetic inputs could incorporate heart rate variability analyses, which use power spectral methods to separate cardiac signals into frequency bands. These can provide more detailed insight that heart rate alone can[46]. Further detailed mapping of the intracardiac nervous system, together with functional imaging of neural networks would also provide insight into roles and anatomical locations of these additional neural networks.

Plasticity and sensory integration in HSPD

The effect of different stimulation protocols were assessed to determine how temporal patterns of stimulation affect HSPD. Repeated stimulation at 5-minute intervals tested whether temporally spaced stimuli leads to habituation or sensitisation. Multiple stimuli in quick succession tested whether HSPD reflect cumulative integration of stimulation, given the findings that response magnitude increases with stimulus strength. Continuous stimulation assessed whether sustained, recurrent stimulation leads to

habituation or sensitisation, observed as a reduction in HSPD magnitude over time, and whether delayed responses such as delayed tachycardia occur, as observed in zebrafish and mammals following the immediate stimulus-induced bradycardia[7,18–20].

HSPD was strongly shaped by sensory integration. Delivering multiple stimuli in quick succession increased the response magnitude, indicating that HSPD scales with cumulative sensory input (Fig. 5B). However, this relationship was not linear in younger embryos. This may reflect immature sensory integration systems or greater variability between individuals.

HSPD also showed experience-dependent plasticity. During repeated stimulation at 10-second intervals over 20 minutes, embryos initially showed strong suppression of cardiac activity. This was followed by an increase in activity as the heart resumed beating despite continued stimulation. This indicated that embryos were habituating, becoming more familiar and less responsive to stimuli. Younger embryos habituated more rapidly, suggesting developmental regulation of the extent and rate of habituation. Notably, a delayed tachycardia was not observed within 5 minutes after stopping stimulation, despite reports in zebrafish and mammals that stimulus-induced bradycardia is followed by a delayed tachycardia[7,18–20]. Potentially, a delayed tachycardia could occur later than this recording period, requiring longer monitoring to detect.

Similar reductions in response were observed with longer (5 minute) intervals between repeated stimulation. While progressive reductions in HR_{50} may reflect longer-term habituation, concurrent reductions in baseline HR indicate that physiological fatigue may also contribute. Compared with the recurring 10-second shocks, habituation here was milder. This may be due to fewer repetitions of stimulation, as habituation could increase with additional repetitions. Alternatively, longer intervals between stimuli may have weakened “memory” of previous stimuli.

These findings demonstrate that HSPD depends on integrated sensory input rather than being a fixed reflexive response. The plasticity and experience-dependence of HSPD suggest that it may be adaptive. The pattern of habituation parallels the startle response, a conserved adaptive, defensive behavior characterized by rapid motor reaction to stimulation, accompanied by cardiac modulation[12]. Like HSPD, startle response is age-dependent, becoming more consistent and amplified with maturation of underlying neural circuits[15,16]. Fish and mammals also become habituated with repeated stimulation[14,17,19,20]. Notably, mechanical stimulation often induced embryo rotation within the chorion alongside HSPD, consistent with motor startle responses.

However, despite similarities, HSPD appears to be mechanically distinct. Unlike the startle response, HSPD was unaffected by neuromuscular blockade[15,47,48]. Furthermore, HSPD involves prolonged cardiac arrest rather than the transient bradycardia associated with startle responses[7,18]. These differences imply that while HSPD and startle response may share sensory pathways, they diverge downstream to produce distinct outputs. Quantifying movements induced by varying strengths and frequencies of stimulation alongside HSPD could provide insight into whether cardiac and motor responses are independently or co-regulated, and how these behaviours develop and interact.

Potential adaptive functions of HSPD

The absence of HSPD in dechorionated embryos suggests it is only important while confined to the chorion, becoming unnecessary after hatching. Embryos are particularly vulnerable during diapause, often residing out of the water[29,30]. Inside the chorion, embryos are unable to swim away from predators, and their heart beats may create vibrations detectable by small predators. By temporarily stopping their heart beating when they sense movement, they reduce these signals, thereby reducing detectability. Post-hatching the response was lost, but embryos can swim. This implies HSPD is important during the embryonic period and developmentally regulated.

Post-hatching, stimulus-induced changes in cardiac activity differed to HSPD. Although prolonged heart stops no longer occurred, touch induced a much more transient bradycardia (Fig. 7) and rapid movement, similar to startle responses in zebrafish[7,18]. Sensitivity was greatest at the head and decreased towards the tail, likely reflecting differences in mechanosensory neurons (e.g. trigeminal neurons in the head, Rohon-Beard in the trunk and tail), which are also known to elicit different motor responses in zebrafish[15].

Conclusions, future directions & limitations

This work provides insight into the neurotransmitter systems and cardiac innervation associated with HSPD. It also reveals the plasticity and potential functional significance of the response, including and how sensory input shapes it. These findings are insightful and establish a foundation for future mechanistic studies. However, they also raise new questions and avenues for investigation.

Overall, this study demonstrates that HSPD is a developmentally regulated, nervous system mediated, and plastic cardiac response that likely serves an adaptive anti-predation role in embryonic survival. Mechanical stimuli are detected by sensory neurons, with integration of sensory information involving complex autonomic interactions. The response is dependent on developmental stage and is shaped by prior experience. Together, these show that HSPD is not a simple fixed reflex, but a coordinated, context-dependent response, reflecting the integration of complex autonomic neural pathways.

Declarations

Ethical declaration

All experiments and methods were performed in accordance with the relevant guidelines and regulations of UK Home Office with the license number PP4402521. All methods are reported in accordance with ARRIVE guidelines. All experiments and methods approved by the Animal Welfare and Ethical Review Board (AWERB) at the University of Exeter.

Resource availability

Materials Availability

No new reagents were generated in this study.

Data and Code Availability

The research data and Pixel Variance code supporting this publication are openly available from the University of Exeter's institutional repository (ORE) at https://doi.org/10.24378/exe.5506. A description of the Pixel Variance algorithm is given in reference [49].

Acknowledgements

TK is funded by NC3Rs project grant (NC/X001121/1). RH was funded by University of Exeter – Employer Engagement & Student Employment (EESE). We thank Sulayman Mourabit, Thomas Cosgrove, Rachel Osman, Clare Bushell, Ed Grinsted, Maryia Fralova and Matt Winter for their support. We also thank Aquatic Resource Centre staff for fish husbandry and to Biosciences teaching lab staff for sharing the lab space and equipment.

Author Contributions

Conceptualization TK, Data curation RH, Investigation RH, Methodology TK, ADC, RH, Writing – original draft RH, TK, Writing – review & editing RH, TK, ADC

Declaration of interests

The authors declare no competing interests.

Methods

EXPERIMENTAL MODEL AND STUDY PARTICIPANT DETAILS

Mangrove killifish source and husbandry

The mangrove killifish *Kryptolebias marmoratus* wild type Hon9 line[40] was sourced and maintained in the Aquatic Resource Centre at the University of Exeter. These fish were kept in a recirculation system under artificial photo periods of 14 hours of light to 10 hours of darkness. All fish were hermaphrodites.

Embryo collection/incubation

For this study, the *K. marmoratus* Hon9 line[40] was used. Embryos were incubated at 28°C in 14.6ppt artificial brackish water. Water changes were made every other day. Embryos were aged according to the Mourabit *et al.,* 2011 staging reference[31]. Embryos used for this study were ages 7 to 20dpf.

METHOD DETAILS

Imaging

Movies were recorded using the digital microscope Jiusion 2K HD 2560x1440P USB Digital Microscope VirtualDub[50] in .avi format. For anatomy imaging, Nikon SMZ1500 and Digital Sight DS-U2 camera were used.

Mechanical stimulation assay

To administer controlled and reproducible physical stimuli to embryos held in a petri dish, a pendulum-based setup was assembled. Agar moulds to hold embryos were prepared using 1% molecular-grade agarose in deionized water in a 6cm petri dish, with a duplex cable wire to form a well to hold embryos. Three embryos were placed in the mould with 14.6ppt water. and positioned under a microscope at the base of a clamp stand (Fig. 1). A small steel ball (4.09g) was strung from a horizontal bar 20cm above the edge of the petri dish. The pendulum could be drawn back to a specified angle and released, hitting the petri dish.

This pendulum-based system was used to induce reproducible mechanical stimulation across experiments. Embryos were transferred to this set-up and left to settle for 5 minutes to allow for recovery from HSPD that may have occurred from moving embryos before filming. Baseline heart rate (HR) was recorded for 30 seconds. Stimulation was administered by drawing the pendulum back to a specified angle and releasing it to hit the petri dish. Recording continued for 90 seconds to capture recovery.

Effect of stimulus strength

First, to assess whether the size of shock impacted HSPD, embryos aged 10-14dpf (*n*=9 for each age) were subjected to the mechanical stimulation assay, stimulated using a range of release angles (10-40°). Having tested this, a release from an angle of 20° was selected to use for remaining analyses, equating to a momentum of 1.989×10^{-3} kg·m/s. This stimulus induced HSPD without causing embryos to shift within their chorions, which sometimes occurred at higher momentums, making image analysis difficult.

HSPD throughtout development

Embryos were filmed for 120s, 25s into the movie the pendulum was released to hit the petri dish, inducing HSPD. Embryos aged 7-20dpf were used (*n*=9 for each age).

Effect of light

To assess whether embryos were also responsive to light stimulation, three embryos were placed under the microscope with the light off. Embryos were filmed for 60s, and 25s into the movie the microscope light was switched on.

Pharmacological treatments

Seven compounds affecting autonomic, neuromuscular or neurotransmitter systems were selected[51–56] (table 3) to test on 12 dpf embryos, when HSPD responses are stable[57]. Starting working concentrations used were mostly based on zebrafish studies. *K. marmoratus* require higher concentrations and longer incubation periods due to their larger size. Therefore, higher concentrations were required for most drugs. Atropine and propranolol Initial concentrations were based on zebrafish studies[51]. These caused observable effects so were used as the working concentrations. Similarly, tricaine initial concentrations had observable effect (lack of jaw and fin movement) so was used as the working concentration. Initial concentrations for 2-phenoxyethanol, dizocilpine, gabazine, were based on zebrafish studies[52–54], while ketanserin concentration was based on previous *K. marmoratus* studies[55]. Concentrations were increased

incrementally until consistent effects on HR_{50} were observed across all fish. Tubocuarine concentration was based on zebrafish studies[56]. Concentrations were increased incrementally until movement was no longer observed in response to touching embryos with tweezers, indicating sufficient paralysis. Stock and working concentrations, incubation times and solvents are provided in Supplementary Table 1. All stocks were diluted into brackish water for bath application.

Stimulus effects

To assess stimulus integration and plasticity during development, embryos (9-13 dpf) were tested under three systems using pendulum-based stimulation.

Stimulation repeated at 5-minute intervals: Embryos received stimulation following 30 seconds baseline recording. Recording continued for 90 seconds post-stimulation. This was repeated five times per group, 5 minutes apart.

Multiple successive stimuli: Embryos received 1-3 stimuli, 5 seconds apart following 30 seconds baseline recording. Recording continued for 90 seconds post-stimulation.

Continuous stimulation: Embryos received stimuli every 10 seconds for 20 minutes, following a 30 second baseline recording period. Cardiac activity was recorded again for 1 minute, starting 5 minutes after the end of stimulation.

Dechorionation & HSPD in dechorionated embryos

To assess how region-specific stimulation affects HSPD, 12 dpf embryos were dechorionated to enable direct tactile stimulation to defined body regions. Dechorionation was performed following established protocols[58], modified for *K. marmoratus*. Hatching enzyme was extracted from homogenised 11 dpf *Aphanius dispar* embryos, due to limited availability of *K. marmoratus*. Homogenates were incubated in a rotator overnight at 4°C, centrifuged at 13000 rpm for 10 minutes, then supernatants diluted 1:1 in brackish water and stored at -20°C. For dechorionation, *K. marmoratus* embryos were gently rubbed on P2000 sandpaper (~1 minute), incubated with Pronase (8 mg/mL) at 28°C (1 hour), washed, and incubated with hatching enzyme at 28°C. Dechorionation was typically complete within 2 hours.

Dechorionated embryos were held in an agarose mould, baseline activity was recorded for 30 sections, then a specified region was gently touched with a needle. Recording continued for 90 seconds to capture recovery. To confirm responses were not stimulus-specific, dechorionated embryos were also tested using pendulum-based stimulation.

Drug	Broad classification	Mechanism	Known Effect(s) on Cardiac Activity
2-Phenoxyethanol	Anaesthetic	–	HR reduced[59,60]
Tricaine	Anaesthetic	Blocks sodium ion channels in nerve cells, preventing initiation or transmission of signals	Dose dependent reductions in HR in zebrafish embryos[61,62] and adults[17,63], little effect on in frogs HR but increase variability[64,65]
Tubocurarine	Neuromuscular blocker	Nicotinic acetylcholine receptor antagonist	HR either increased[66,67] or unaffected[68,69], blood[66] and arterial[67] pressure reduced, cardiac output reduced[66]
Atropine	ANS modulator (PSNS inhibitor)	Muscarinic acetylcholine receptor antagonist (cholinergic antagonist)	Doses dependent effects: low doses may cause bradycardia, moderate-high doses tachycardia[70,71]
Propranolol	ANS modulator (SNS inhibitor)	β-adrenoreceptor antagonist (epinephrine and norepinephrine blocker)	HR reduced[72–74]
Dizocilpine (MK-801)	Neurotransmitter antagonist	Glutamatergic (NMDA receptor) antagonist	HR unaffected[75,76]
Gabazine	Neurotransmitter antagonist	GABAergic antagonist	Transient mild increase in HR[77,78]
Ketanserin	Neurotransmitter antagonist	Serotonergic antagonist	Transient reduction in blood pressure, HR unaffected[79]

Table 3. Pharmacological agents used in this study, classifications, mechanisms, and previously reported effects on cardiac activity.

QUANTIFICATION AND STATISTICAL ANALYSIS

Cardiac activity extraction

Heart rate, stopping and recovery analysis

All videos using the mechanical stimulation assay, as well as touching experiments with dechorionated embryos were analysed. ImageJ[80] was used to select the ROI over a single chamber, convert to 8-bit greyscale and export to a TIF image sequence. This image sequence was analysed using a 'Pixel Variance' algorithm which has been previously applied to the contraction of cardiomyocyte monolayers[49]. In short,

the algorithm calculates the variance in the pixel value across frames captured over a known time interval. This time interval corresponds to ~40% of the beat period, i.e. 0.4 seconds for the resting 1 Hz heart rate, equivalent to two frames when sampling at 5.7 fps. Once the variance has been calculated on a pixel-wise basis, the value is averaged across all the pixels in the region of interest (ROI). A trace of this value over time provides a measure of the speed with which the pixel values are changing. For a single beat, there will be two peaks in the speed profile, corresponding to contraction and relaxation. The baseline value of the contraction speed varies between ROIs and samples due to the presence of local features and differences in average intensity. Peaks in the 'contraction speed' traces were then identified using the peak prominence (typically >50% of the peak height) relative to the baseline rather than hardcoding the absolute peak height.

Once the timing of the individual peaks had been identified, the number of peaks within five second windows (starting from time zero) were calculated and divided by two to obtain the number of complete heart beats per five second interval. This 'beat count' data, averaged over a five second window, was attributed to the midpoint of the window (i.e. 2.5, 7.5, 12.5 etc. seconds).

Baseline heart rate was calculated for each embryo using pre-stimulus beat count data. Averages and standard deviation were then calculated for each age. For each embryo, the time taken for heart rate to recover to 50% of the pre-stimulus rate was measured. The first point of recovery considered was the timepoint 2.5s post-stimulation, as the 0s timepoint was not an accurate representation, due to the noise in data following the mechanical stimulation which often caused the embryos to slightly rotate inside the chorion. For this reason, very short heart stops were not captured.

Contraction profiles of individual chambers

ImageJ was used to select a ROI over the sinus venosus, atrium and ventricle separately and plot separate z-axis profiles. Data points were extracted and plotted on a single graph for each movie. Drift was removed using a Butterworth high-pass filter, with zero-phase delay.

For three embryos, the durations between contractions of individual chambers were measured. For each embryo, four measurements were taken before HSPD and four after. The Wilcoxon signed-rank test was then used for each embryo to compare the timing between chamber contractions before and after HSPD.

Statistical analysis

Normality was assessed using Shapiro-Wilk tests in MATLAB to inform selection of statistical tests, with significance threshold $p<0.05$. Cardiac activity was primarily quantified using baseline HR, calculated as the mean rate for the 30 seconds preceding stimulation; and recovery metric HR_{50}, defined as time to return to 50% of baseline HR post-stimulation.

Influence of shock strength on HSPD

Using movies stimulating embryos with varying pendulum release angles, the influence of increasing stimulus momenta on HSPD was quantified. The time from administration of the stimulus to the first

heartbeat following HSPD was timed. Averages and standard deviation were calculated for each age and release angle.

Control / HSPD throughout development

Averages and standard deviation for time to reach 50% recovery were then taken for each dpf. The Mann-Whitney U-test was used to compare heart rates for each age in the “developing” category (7–13dpf) to the “diapause” category (14–20dpf). The Mann-Whitney U-test was also used to compare heart rates between untreated and tricaine treated embryos for individual ages.

Pharmacological treatments

Drug effects on HR and HR_{50} were assessed using Wilcoxon rank-sum, relative to control. As some groups significantly deviated from normality (W=0.70–0.74, p<0.005), non-parametric tests were used.

Continuous stimulation

Cardiac activity was quantified using beat counts per 10-second interval (BC10s) (Supp. fig. 4). As stimuli during the stimulation period were administered every 10 seconds, BC10s values were used to make a time-series across the 20-minute stimulation period. Baseline was defined as the mean BC10s across the 30 seconds preceding stimulation. The following metrics were extracted from these: Minimum BC10s – the minimum BC10s value in the timeseries; time to minimum – time from stimulation onset to minimum BC10s; and relative drop – percentage decrease in BC10s to baseline.

To characterise temporal changes, mean BC10s values were taken from four windows across the experiment. Means for each age were calculated and analysed using a repeated-measures Friedman test with post hoc pairwise comparisons against baseline.

To characterise habituation (i.e. return of cardiac activity with reduced responsiveness to repeated stimulation), the timeseries from the first occurrence of the minimum BC10s value onwards were fitted with a linear regression:

$$BC10s(t) = m\,t + c$$

where t represents time (minutes) since the minimum BC10s, m is the recovery slope, and c is the fitted BC10s value at the start of the post-minimum response period. Model fit was assessed using the coefficient of determination (R^2) and root mean square error (RMSE).

HSPD in dechorionated embryos

Given the absence of HSPD, cardiac output in touching experiments was quantified using inter-beat interval (IBI), defined as the time (seconds) between two beats. Baseline IBIs were calculated as average IBI for the 30 seconds of recording preceding stimulation. Due to variability between fish, IBI were normalised to baseline. Grouped by touch location, normalised post-stimulus IBIs were compared to baseline using t-tests.

For dechorionated embryos tested with pendulum stimulation, t-tests were used to compare dechorionated to control.

References

1. Gao R, Ren J (2021) Zebrafish Models in Therapeutic Research of Cardiac Conduction Disease. Front Cell Dev Biology 9. 10.3389/fcell.2021.731402
2. Gordan R, Gwathmey JK, Xie LH (2015) Autonomic and endocrine control of cardiovascular function. World J Cardiol 7(4):204–214. 10.4330/wjc.v7i4.204 PubMed PMID: 25914789; PubMed Central PMCID: PMC4404375
3. van Weerd JH, Christoffels VM (2016) The formation and function of the cardiac conduction system. Development 143(2):197–210. 10.1242/dev.124883
4. Stoyek MR, Croll RP, Smith FM (2015) Intrinsic and extrinsic innervation of the heart in zebrafish (Danio rerio). J Comp Neurol 523(11):1683–1700. 10.1002/cne.23764
5. Mani BC, Pavri BB (2014) Dual Atrioventricular Nodal Pathways Physiology: A Review of Relevant Anatomy, Electrophysiology, and Electrocardiographic Manifestations. Indian Pacing Electrophys J 14(1):12–25. 10.1016/S0972-6292(16)30711-2
6. Pappano AJ, Gil Wier W (2013) Regulation of the Heartbeat. Cardiovascular Physiology. Elsevier, pp 91–118. doi:10.1016/B978-0-323-08697-4.00005-8
7. Stoyek MR, Quinn TA, Croll RP, Smith FM (2016) Zebrafish heart as a model to study the integrative autonomic control of pacemaker function. Am J Physiol Heart Circ Physiol 311(3):H676–H688. 10.1152/ajpheart.00330.2016
8. Franciosi S, Perry FKG, Roston TM, Armstrong KR, Claydon VE, Sanatani S (2017) The role of the autonomic nervous system in arrhythmias and sudden cardiac death. Auton Neurosci 205:1–11. 10.1016/j.autneu.2017.03.005
9. Végh AMD, Duim SN, Smits AM, Poelmann RE, ten Harkel ADJ, DeRuiter MC et al (2016) Part and Parcel of the Cardiac Autonomic Nerve System: Unravelling Its Cellular Building Blocks during Development. J Cardiovasc Dev Disease 3(3):28. 10.3390/jcdd3030028 PubMed PMID: 29367572; PubMed Central PMCID: PMC5715672
10. Pedroni A, Yilmaz E, Del Vecchio L, Bhattarai P, Vidal IT, Dai YWE et al (2024) Decoding the molecular, cellular, and functional heterogeneity of zebrafish intracardiac nervous system. Nat Commun 15(1):10483. 10.1038/s41467-024-54830-w
11. Srinivasan NT, Schilling RJ (2018) Sudden Cardiac Death and Arrhythmias. Arrhythmia. Electrophysiol Rev 7(2):111–117. 10.15420/aer2018:15:2 PubMed PMID: 29967683; PubMed Central PMCID: PMC6020177
12. Koch M (1999) The neurobiology of startle. Prog Neurobiol 59(2):107–128. 10.1016/S0301-0082(98)00098-7
13. Zheng A, Schmid S (2023) A review of the neural basis underlying the acoustic startle response with a focus on recent developments in mammals. Neurosci Biobehavioral Reviews 148:105129.

10.1016/j.neubiorev.2023.105129

14. Faria M, Prats E, Novoa-Luna KA, Bedrossiantz J, Gómez-Canela C, Gómez-Oliván LM et al (2019) Development of a vibrational startle response assay for screening environmental pollutants and drugs impairing predator avoidance. Sci Total Environ 650:87–96. 10.1016/j.scitotenv.2018.08.421
15. Saint-Amant L, Drapeau P (1998) Time course of the development of motor behaviors in the zebrafish embryo. J Neurobiol 37(4):622–632. 10.1002/(SICI)1097-4695(199812)37:4%3C622::AID-NEU10%3E3.0.CO;2-S
16. Hernandez-Nunez L, Avrami J, Shi S, Markarian A, Boulanger-Weill J, Zarghani-Shiraz A et al (2025) Emergence of Functional Heart-Brain Circuits in a Vertebrate. bioRxiv. 2025.09.22.677693. doi:10.1101/2025.09.22.677693
17. Mann KD, Hoyt C, Feldman S, Blunt L, Raymond A, Page-McCaw PS (2010) Cardiac response to startle stimuli in larval zebrafish: sympathetic and parasympathetic components. Am J Physiology-Regulatory Integr Comp Physiol 298(5):R1288–R1297. 10.1152/ajpregu.00302.2009
18. Smith FM (2023) Fundamental Neurocardiology: The Intracardiac Nervous System. In: Tripathi ON, Quinn TA, Ravens U (eds) Heart Rate and Rhythm: Molecular Basis, Pharmacological Modulation and Clinical Implications. Springer International Publishing, Cham, pp 151–186. doi:10.1007/978-3-031-33588-4_8
19. Casto R, Nguyen T, Printz MP (1989) Characterization of cardiovascular and behavioral responses to alerting stimuli in rats. Am J Physiol 256(5):R1121–1126. 10.1152/ajpregu.1989.256.5.R1121 PubMed PMID: 2719154
20. Holand S, Girard A, Laude D, Meyer-Bisch C, Elghozi JL (1999) Effects of an auditory startle stimulus on blood pressure and heart rate in humans. J Hypertens 17(12):1893
21. Thompson R (2001) Habituation. International Encyclopedia of the Social & Behavioral Sciences. Elsevier, pp 6458–6462. doi:10.1016/B0-08-043076-7/03639-1
22. Fendt M, Koch M, Schnitzler HU, Pharmacology (1994) Biochem Behav 48(2):307–314. 10.1016/0091-3057(94)90532-0 PubMed PMID: 7916463
23. Koch M, Ebert U (1993) Enhancement of the acoustic startle response by stimulation of an excitatory pathway from the central amygdala/basal nucleus of Meynert to the pontine reticular formation. Exp Brain Res 93(2):231–241. 10.1007/BF00228390 PubMed PMID: 8491264
24. Roberts AC, Alzagatiti JB, Ly DT, Chornak JM, Ma Y, Razee A et al (2020) Induction of Short-Term Sensitization by an Aversive Chemical Stimulus in Zebrafish Larvae. eNeuro 7(6). 10.1523/ENEURO.0336-192020 PubMed PMID: 33004417
25. Shen MJ, Zipes DP (2014) Role of the Autonomic Nervous System in Modulating Cardiac Arrhythmias. Circul Res 114(6):1004–1021. 10.1161/CIRCRESAHA.113.302549
26. King JAC, Abel DC, DiBona DR (1989) Effects of salinity on chloride cells in the euryhaline cyprinodontid fish Rivulus marmoratus. Cell Tissue Res 257(2):367–377. 10.1007/BF00261839
27. Taylor DS (1990) Adaptive Specializations of the Cyprinodont Fish Rivulus Marmoratus. Fla Sci 53(3):239–248

28. Taylor S, Davis W, m. P, Turner B (1995) Rivulus Marmoratus: Ecology of Distributional Patterns in Florida and the Central Indian River Lagoon. Bull Mar Sci 57:202–207
29. Ritchie SA, Davis WP (1986) Evidence for embryonic diapause in Rivulus marmoratus: laboratory and field observations. J Am Killifish Association 19:103–108
30. Karp X (2021) Hormonal Regulation of Diapause and Development in Nematodes, Insects, and Fishes. Front Ecol Evol 9. 10.3389/fevo.2021.735924
31. Mourabit S, Edenbrow M, Croft DP, Kudoh T (2011) Embryonic development of the self-fertilizing mangrove killifish Kryptolebias marmoratus. Dev Dyn 240(7):1694–1704. 10.1002/dvdy.22668
32. Storey KB, Storey JM (1988) Freeze tolerance in animals. Physiol Rev 68(1):27–84. 10.1152/physrev.1988.68.1.27 PubMed PMID: 3275942
33. Layne JR, Lee RE, Heil TL (1989) Freezing-induced changes in the heart rate of wood frogs (Rana sylvatica). Am J Physiology-Regulatory Integr Comp Physiol 257(5):R1046–R1049. 10.1152/ajpregu.1989.257.5.R1046
34. Hanna P, Ardell L, Shivkumar J (2020) Cardiac Neuroanatomy for the Cardiac Electrophysiologist. J Atr Fibrillation 13(1):2407. 104022/jafib.2407 PubMed PMID: 33024507; PubMed Central PMCID: PMC7533134
35. Stoyek MR, Hortells L, Quinn TA (2021) From Mice to Mainframes: Experimental Models for Investigation of the Intracardiac Nervous System. J Cardiovasc Dev Disease 8(11):149. 10.3390/jcdd8110149
36. Kambule IN, Hanrahan SA, Duncan FD (2011) Metabolic rate in diapause and nondiapause brown locust eggs correlated with embryonic development. Physiol Entomol 36(4):299–308. 10.1111/j.1365-3032.2011.00792.x
37. Furness AI, Reznick DN, Tatarenkov A, Avise JC (2018) The evolution of diapause in Rivulus (Laimosemion). Zool J Linn Soc 184(3):773–790. 10.1093/zoolinnean/zly021
38. Podrabsky JE, Riggs CL, Romney AL, Woll SC, Wagner JT, Culpepper KM et al (2017) Embryonic development of the annual killifish Austrofundulus limnaeus: An emerging model for ecological and evolutionary developmental biology research and instruction. Dev Dyn 246(11):779–801. 10.1002/dvdy.24513
39. Hu CK, Wang W, Brind'Amour J, Singh PP, Reeves GA, Lorincz MC et al (2020) Vertebrate diapause preserves organisms long term through Polycomb complex members. Science 367(6480):870–874. 10.1126/science.aaw2601
40. Tatarenkov A, Ring BC, Elder JF, Bechler DL, Avise JC (2010) Genetic Composition of Laboratory Stocks of the Self-Fertilizing Fish Kryptolebias marmoratus: A Valuable Resource for Experimental Research. PLoS ONE 5(9):e12863. 10.1371/journal.pone.0012863
41. Tessadori F, van Weerd JH, Burkhard SB, Verkerk AO, de Pater E, Boukens BJ et al (2012) Identification and Functional Characterization of Cardiac Pacemaker Cells in Zebrafish. PLoS ONE 7(10):e47644. 10.1371/journal.pone.0047644 PubMed PMID: 23077655; PubMed Central PMCID: PMC3473062
42. Šolc D (2007) The heart and heart conducting system in the kingdom of animals: A comparative approach to its evolution. Exp Clin Cardiol 12(3):113–118 PubMed PMID: 18650991; PubMed Central

PMCID: PMC2323757

43. Jensen B, Boukens BJD, Wang T, Moorman AFM, Christoffels VM (2014) Evolution of the Sinus Venosus from Fish to Human. J Cardiovasc Dev Disease 1(1):14–28. 10.3390/jcdd1010014
44. Sridharan A, Bradfield JS, Shivkumar K, Ajijola OA (2022) Autonomic nervous system and arrhythmias in structural heart disease. Auton Neurosci 243:103037. 10.1016/j.autneu.2022.103037
45. Manolis AA, Manolis TA, Apostolopoulos EJ, Apostolaki NE, Melita H, Manolis AS (2021) The role of the autonomic nervous system in cardiac arrhythmias: The neuro-cardiac axis, more foe than friend? Trends Cardiovasc Med 31(5):290–302. 10.1016/j.tcm.2020.04.011
46. Watanabe-Asaka T, Niihori M, Sonobe H, Igarashi K, Oda S, Iwasaki K, ichi et al (2022) Acquirement of the autonomic nervous system modulation evaluated by heart rate variability in medaka (Oryzias latipes). PLoS ONE 17(12):e0273064. 10.1371/journal.pone.0273064 PubMed PMID: 36584168; PubMed Central PMCID: PMC9803310
47. Burr SA, Leung YL (2014) Curare (d-Tubocurarine). Encyclopedia of Toxicology. Elsevier, pp 1088–1089. doi:10.1016/B978-0-12-386454-3.00482-6
48. Norekian TP (1997) Coordination of Startle and Swimming Neural Systems in the Pteropod Mollusk *Clione limacina*: Role of the Cerebral Cholinergic Interneuron. J Neurophysiol 78(1):308–320. 10.1152/jn.1997.78.1.308
49. Corbett AD, Horsell D, Watters T, Ghasemi M, Henderson L, Mohanan S et al Automated measurement of cardiomyocyte monolayer contraction using the Exeter Multiscope [Internet]. bioRxiv; 2024 [cited 2024 Oct 27]. p. 2024.09.09.611998. Available from: https://www.biorxiv.org/content/10.1101/2024.09.09.611998v2 doi:10.1101/2024.09.09.611998
50. Lee A, VirtualDub (2013) [Software]. Version 1.10.4 (Build 35491). Available from: http://www.virtualdub.org
51. Dyballa S, Miñana R, Rubio-Brotons M, Cornet C, Pederzani T, Escaramis G et al (2019) Comparison of Zebrafish Larvae and hiPSC Cardiomyocytes for Predicting Drug-Induced Cardiotoxicity in Humans. Toxicol Sci 171(2):283–295. 10.1093/toxsci/kfz165
52. Dimitriadou S, Miller M, Pilehvar A, Sneddon LU, Bamsey JL, Hogan-Bassey D et al (2025) Evaluating anaesthetics for improving scientific research and welfare using larval zebrafish. bioRxiv; p. 2025.10.06.680636. doi:10.1101/2025.10.06.680636
53. Sison M, Gerlai R (2011) Behavioral performance altering effects of MK-801 in zebrafish (*Danio rerio*). Behav Brain Res 220(2):331–337. 10.1016/j.bbr.2011.02.019
54. Jha U, Kondrychyn I, Korzh V, Thirumalai V (2021) High Behavioral Variability Mediated by Altered Neuronal Excitability in auts2 Mutant Zebrafish. eNeuro 8(5). 10.1523/ENEURO.0493-202021 PubMed PMID: 34544758
55. Regan KS, Jonz MG, Wright PA (2011) Neuroepithelial cells and the hypoxia emersion response in the amphibious fish Kryptolebias marmoratus. J Exp Biol 214(15):2560–2568. 10.1242/jeb.056333
56. Winter MJ, Windell D, Metz J, Matthews P, Pinion J, Brown JT et al (2017) 4-dimensional functional profiling in the convulsant-treated larval zebrafish brain. Sci Rep 7(1):6581. 10.1038/s41598-017-06646-6

57. Herbert R, Corbett AD, Kudoh T (2025) Nervous system mediated cardiac arrest in mangrove killifish. p. 2025.02.03.636252. bioRxiv. doi:10.1101/2025.02.03.636252
58. Porazinski SR, Wang H, Furutani-Seiki M (2010) Dechorionation of Medaka Embryos and Cell Transplantation for the Generation of Chimeras. J Visualized Experiments: JoVE. ;(46):2055. doi:10.3791/2055 PubMed PMID: 21206472; PubMed Central PMCID: PMC3159669.
59. Zahl IH, Samuelsen O, Kiessling A (2012) Anaesthesia of farmed fish: implications for welfare. Fish Physiol Biochem 38(1):201–218. 10.1007/s10695-011-9565-1
60. Mitjana O, Bonastre C, Tejedor MT, Garza L, Esteban J, Falceto MV (2018) Simultaneous effect of sex and dose on efficacy of clove oil, tricaine methanesulfonate, 2-phenoxyethanol and propofol as anaesthetics in guppies, *Poecilia reticulata* (Peters). Aquac Res 49(6):2140–2146. 10.1111/are.13668
61. Denvir MA, Tucker CS, Mullins JJ (2008) Systolic and diastolic ventricular function in zebrafish embryos: Influence of norepenephrine, MS-222 and temperature. BMC Biotechnol 8:21. 10.1186/1472-6750-8-21 PubMed PMID: 18304347; PubMed Central PMCID: PMC2291041
62. Dimitriadou S, Miller M, Pilehvar A, Sneddon LU, Bamsey JL, Hogan-Bassey D et al (2026) Evaluating Anesthetics for Improving Scientific Research and Welfare Using Larval Zebrafish. Compr Physiol 16(3):e70174. 10.1002/cph4.70174
63. Huang WC, Hsieh YS, Chen IH, Wang CH, Chang HW, Yang CC et al (2010) Combined use of MS-222 (tricaine) and isoflurane extends anesthesia time and minimizes cardiac rhythm side effects in adult zebrafish. Zebrafish 7(3):297–304. 10.1089/zeb.2010.0653 PubMed PMID: 20807039
64. Lalonde-Robert V, Beaudry F, Vachon P (2012) Pharmacologic Parameters of MS222 and Physiologic Changes in Frogs (Xenopus laevis) After Immersion at Anesthetic Doses. J Am Assoc Lab Anim Sci 51(4):464–468 PubMed PMID: 23043812; PubMed Central PMCID: PMC3400695
65. Lalonde-Robert V, Desgent S, Duss S, Vachon P (2012) Electroencephalographic and Physiologic Changes after Tricaine Methanesulfonate Immersion of African Clawed Frogs (Xenopus laevis). J Am Assoc Lab Anim Sci 51(5):622–627 PubMed PMID: 23312092; PubMed Central PMCID: PMC3447452
66. Booij LH, Edwards RP, Sohn YJ, Miller RD (1980) Cardiovascular and neuromuscular effects of Org NC 45, pancuronium, metocurine, and d-tubocurarine in dogs. Anesth Analg 59(1):26–30 PubMed PMID: 7188662
67. Antonio RP, Philbin DM, Savarese JJ (1979) Comparative Haemodynamic Effects of Tubocurarine and Metocurine in the Dog. Br J Anaesth 51(11):1007–1010. 10.1093/bja/51.11.1007
68. Dhillon SS, Dóró É, Magyary I, Egginton S, Sík A, Müller F (2013) Optimisation of Embryonic and Larval ECG Measurement in Zebrafish for Quantifying the Effect of QT Prolonging Drugs. PLoS ONE 8(4):e60552. 10.1371/journal.pone.0060552
69. Winter MJ, Pinion J, Tochwin A, Takesono A, Ball JS, Grabowski P et al (2021) Functional brain imaging in larval zebrafish for characterising the effects of seizurogenic compounds acting via a range of pharmacological mechanisms. Br J Pharmacol 178(13):2671–2689. 10.1111/bph.15458
70. Montano N, Cogliati C, Porta A, Pagani M, Malliani A, Narkiewicz K et al (1998) Central Vagotonic Effects of Atropine Modulate Spectral Oscillations of Sympathetic Nerve Activity. Circulation 98(14):1394–1399. 10.1161/01.CIR.98.14.1394

71. Das G, Therapeutic (1989) Cardiac effects of atropine in man: an update. Int J Clin Pharmacol Therapy Toxicol 27(10):473–477 PubMed PMID: 2684867
72. van Opbergen CJM, Koopman CD, Kok BJM, Knöpfel T, Renninger SL, Orger MB et al (2018) Optogenetic sensors in the zebrafish heart: a novel in vivo electrophysiological tool to study cardiac arrhythmogenesis. Theranostics 8(17):4750–4764. 10.7150/thno.26108 PubMed PMID: 30279735; PubMed Central PMCID: PMC6160779
73. Finn J, Hui M, Li V, Lorenzi V, De La Paz N, Cheng SH et al (2012) Effects of propranolol on heart rate and development in Japanese medaka (Oryzias latipes) and zebrafish (Danio rerio). Aquat Toxicol 122–123:214–221. 10.1016/j.aquatox.2012.06.013
74. Brink A (1971) Effect of propranolol on the metabolism and function of the rat heart. J Mol Cell Cardiol 2(2):71–89. 10.1016/0022-2828(71)90062-9
75. Tian B, Hartle DK (1994) Cardiovascular effects of NMDA and MK-801 infusion at area postrema and mNTS in rat. Pharmacol Biochem Behav 49(3):489–495. 10.1016/0091-3057(94)90060-4
76. Tian B, Hartle DK (1994) MK-801 affects cardiovascular responses produced by GABAA agents in area postrema. Brain Res Bull 35(1):63–67. 10.1016/0361-9230(94)90217-8 PubMed PMID: 7953759
77. Tjen-A-Looi SC, Guo ZL, Longhurst JC (2014) GABA in nucleus tractus solitarius participates in electroacupuncture modulation of cardiopulmonary bradycardia reflex. Am J Physiology-Regulatory Integr Comp Physiol 307(11):R1313–R1323. 10.1152/ajpregu.00300.2014
78. Jt JZ (2010) Role of GABAergic neurones in the nucleus tractus solitarii in modulation of cardiovascular activity. Exp Physiol 95(9). 10.1113/expphysiol.2010.054007 PubMed PMID: 20591977
79. Davy M, Midol-Monnet M, Heimburger M, Beslot F, Cohen Y (1987) Peripheral and central cardiovascular effects of ketanserin in conscious normotensive rats. Arch Int Pharmacodyn Ther 290(2):193–206 PubMed PMID: 3128194
80. Schneider CA, Rasband WS, Eliceiri KW (2012) NIH Image to ImageJ: 25 years of image analysis. Nat Methods 9(7):671–675. 10.1038/nmeth.2089

Figures

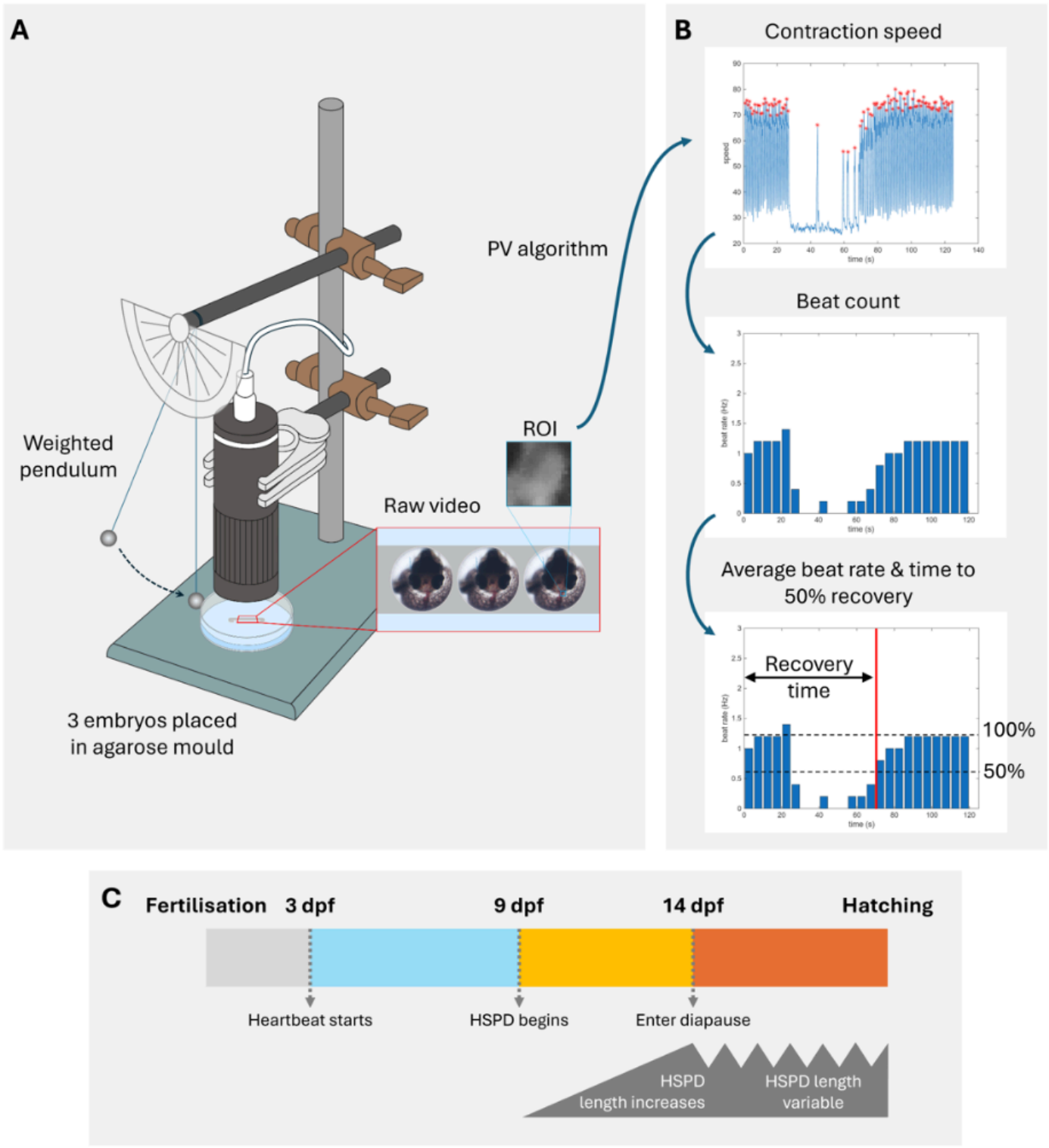

Figure 1

Summary of methods and results. (A) Set-up: embryos were placed in an agarose mold under a microscope, and HSPD was induced and filmed using a pendulum-based mechanical stimulation setup. (B) Data analysis: from the recordings, a region of interest (ROI) was selected over a single heart chamber. The Pixel Variance algorithm was performed to find contraction speed, and beat count was calculated (example shown for 12 dpf). From this, the baseline pre-stimulus average heart rate, and time to 50% recovery after

HSPD were measured. (C) Summary of results: key stages in the development of HSPD from fertilization to hatching (top); grey panel (bottom) illustrates that the duration of HSPD increases from 9 to 14dpf and becomes variable during diapause.

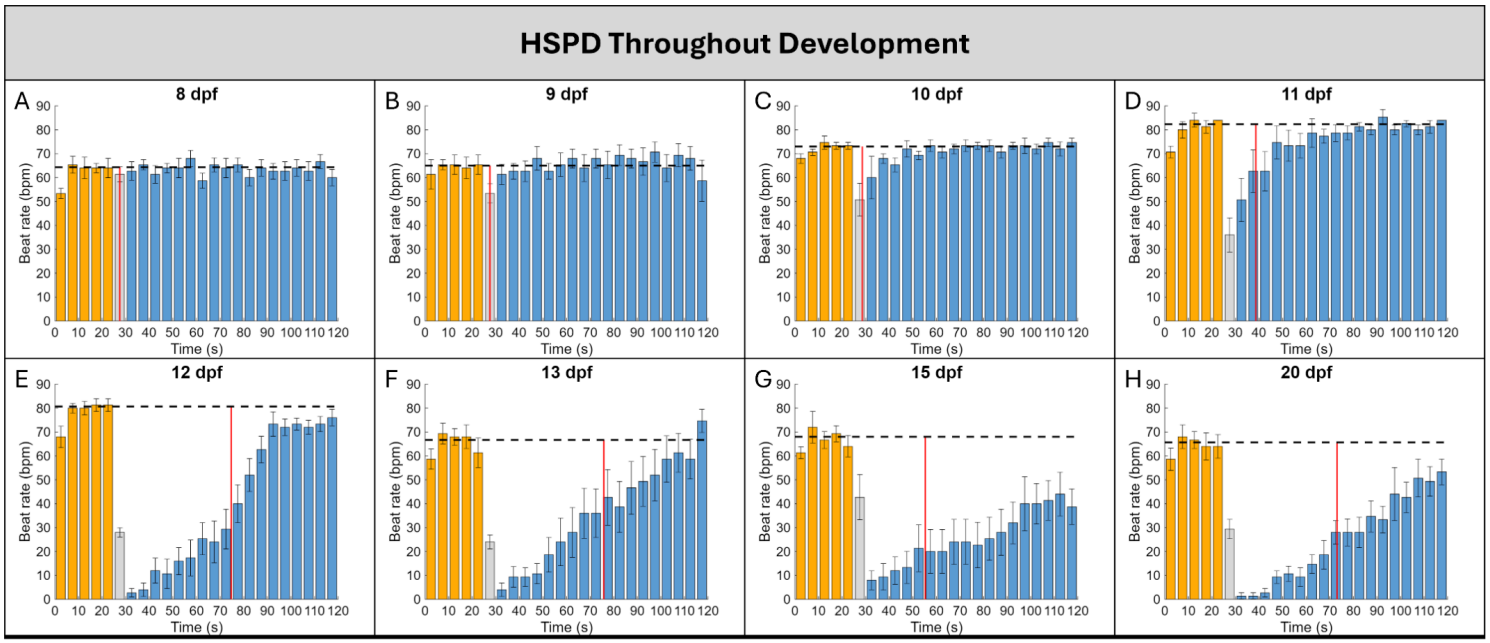

Figure 2

HSPD starts from 9dpf and increases in duration throughout development. Heart rate was measured at 8-13, 15 and 20dpf for untreated embryos at 5-second intervals over 120s movies. At 25s, stimulation was applied, inducing HSPD. Embryos stopped their heart beat in response to the stimulation. Orange bars show heart rate before the stimulus at 25s, from which the baseline pre-stimulus average heart rate was calculated, indicated by the black dotted line. Blue bars show post-stimulus heart rate. Red lines mark the average time at which heart rate reached 50% of the pre-stimulus rate. The time points indicated by grey bars (27.5s) were not included in recovery time due to noise caused by embryo movement following the stimulus. Error bars show SEM.

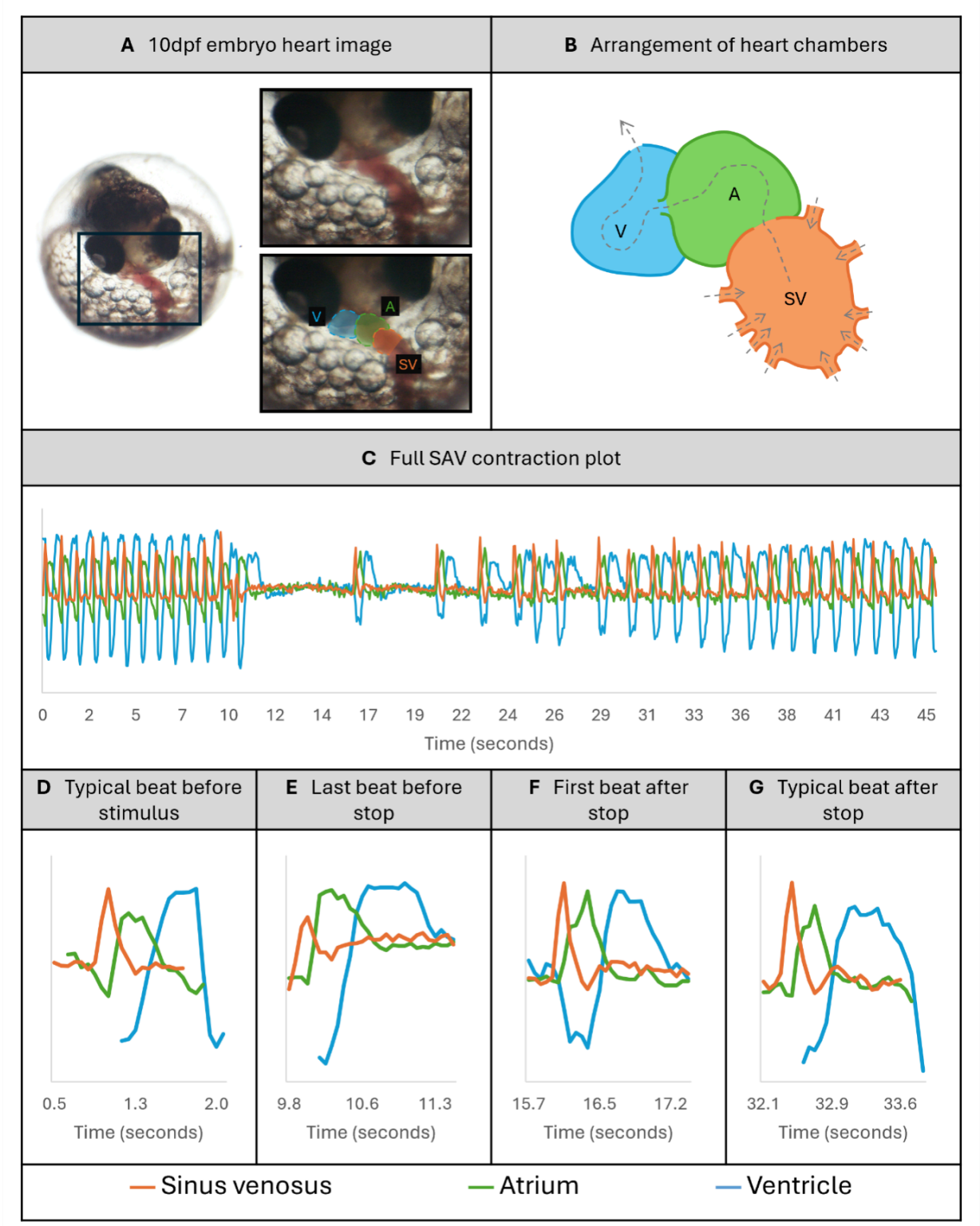

Figure 3

Heart chambers and contraction plots. (A) Image of *K. marmoratus* embryo at 10dpf, once HSPD ability is established. SV (sinus venosus) is indicated in orange, A (atrium) in green, V (ventricle) in blue. (B) Arrangement of chambers, arrows indicating the direction of blood flow. (C) A full SAV (Sinus venosus, Atrium and Ventricle) contraction plot from a 45-second movie of a 12dpf embryo. Physical stimulation was applied at ~10s, inducing HSPD. Below, individual beats are highlighted: (D) a typical beat from before the

stimulus, (E) the last beat before HSPD, (F) the first beat after HSPD and (G) a typical beat after the heart rate recovers. Peaks indicate contractions for each chamber. Lines are coloured according to the chamber.

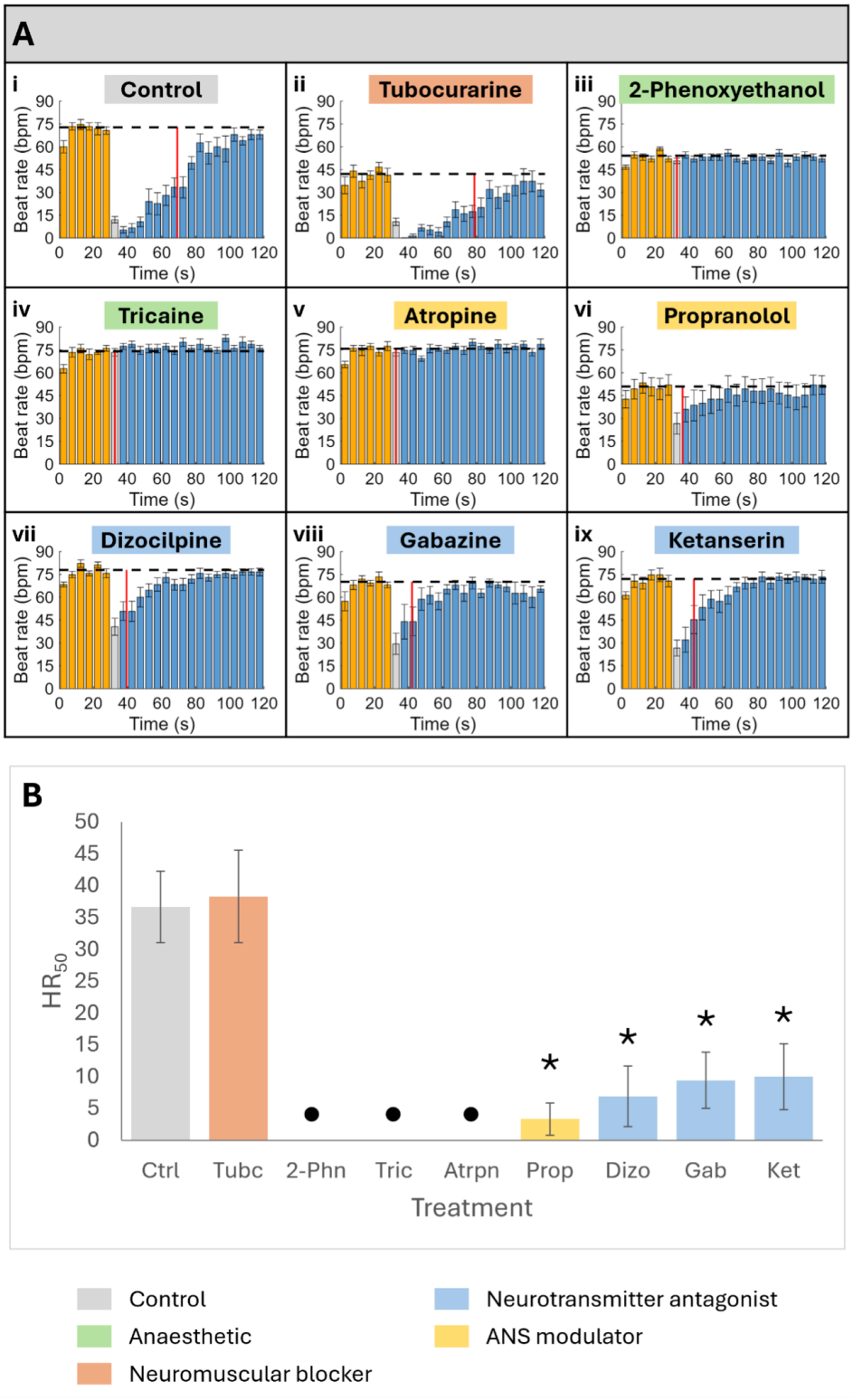

Figure 4

Effects of pharmacological treatments on HSPD in 12 dpf embryos. n=9 per group. **A:** Heart rate measured at 5-second intervals over 120s movies. At 30s, stimulation was applied. Orange bars show heart rate

before the stimulus at 30s, from which the baseline pre-stimulus average heart rate was calculated, indicated by the black dotted line. Blue bars show post-stimulus heart rate. Red lines mark the average time at which heart rate reached 50% of the pre-stimulus rate. The time points indicated by grey bars (32.5s) were not included in recovery time due to noise caused by embryo movement following the stimulus. Error bars show SEM. **B:** mean HR_{50} (time to reach 50% baseline heart rate following stimulation). Error bars show standard deviation. Asterisks (*) indicate values significantly different from control (p<0.05). Dots (•) indicate where HR_{50} values of 0 seconds, reflecting the absence of HSPD, therefore, no recovery period. Colours indicate drug class, as shown in the legend. Ctrl, control; 2-Phn, 2-phenoxyethanol; Tubc, tubocurarine; Atrpn, atropine; Prop, propranolol; Dizo, dizocilpine; Gab, gabazine; Ket, ketanserin.

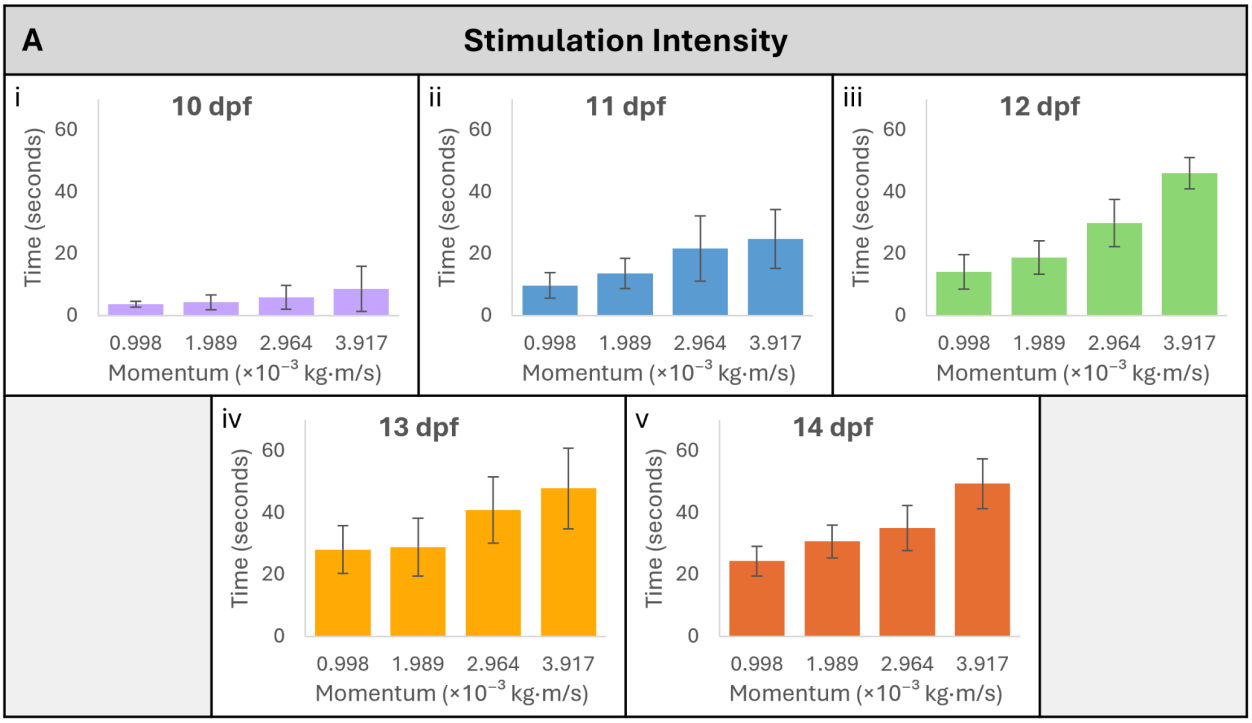

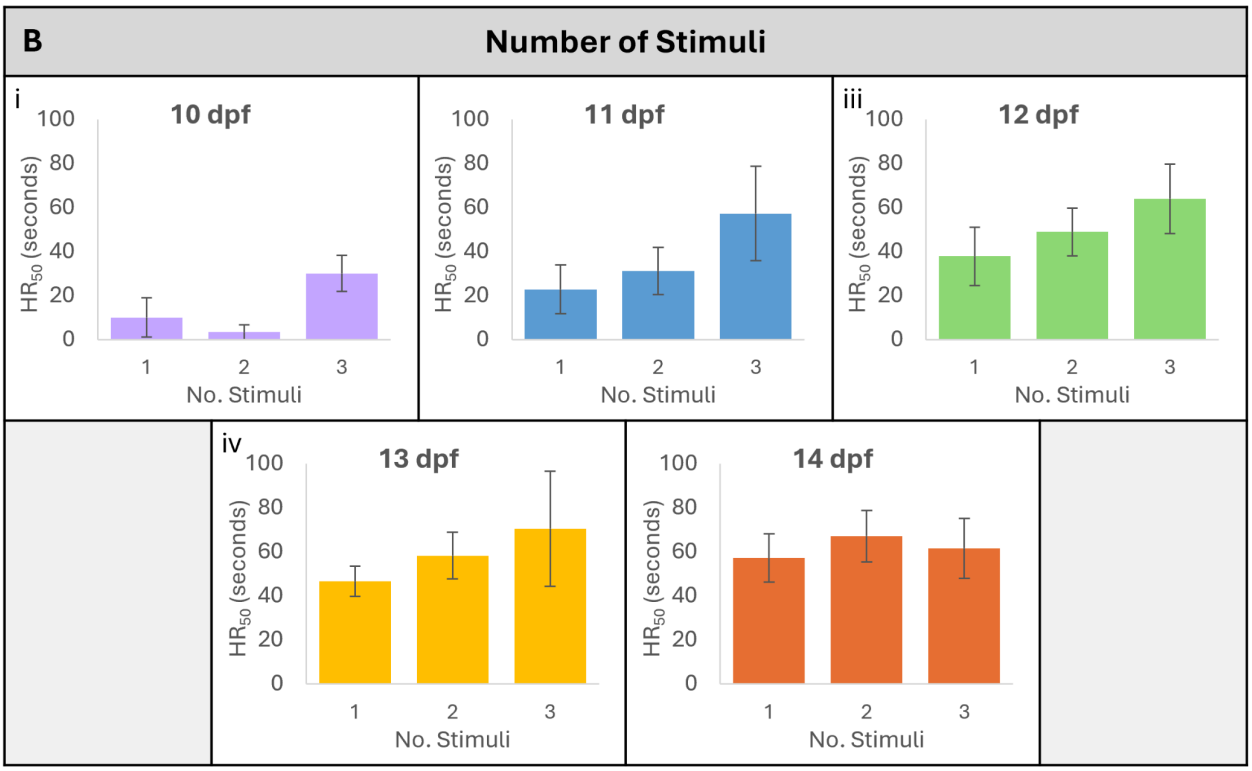

Figure 5

Effect of stimulation intensity and number of stimuli on HSPD. n=9 per group. (A) A range of physical stimuli with varying momentum were applied to *K. marmoratus* 10-14 dpf embryos. With increasing stimulation momentum, the length of heart stops increased, measured by time from the stimulus to the first heartbeat after HSPD. Error bars show standard deviation. (B) Recovery from HSPD following different numbers of stimuli. Embryos 10-14 dpf were recorded for 30s to obtain baseline heart rate, then

administered either 1, 2 or 3 stimuli quick succession – 5 seconds apart. HR_{50} was then calculated as the time to recover to 50% of baseline heart rate after the final stimulus. Bars show mean HR_{50}, error bars show standard deviation.

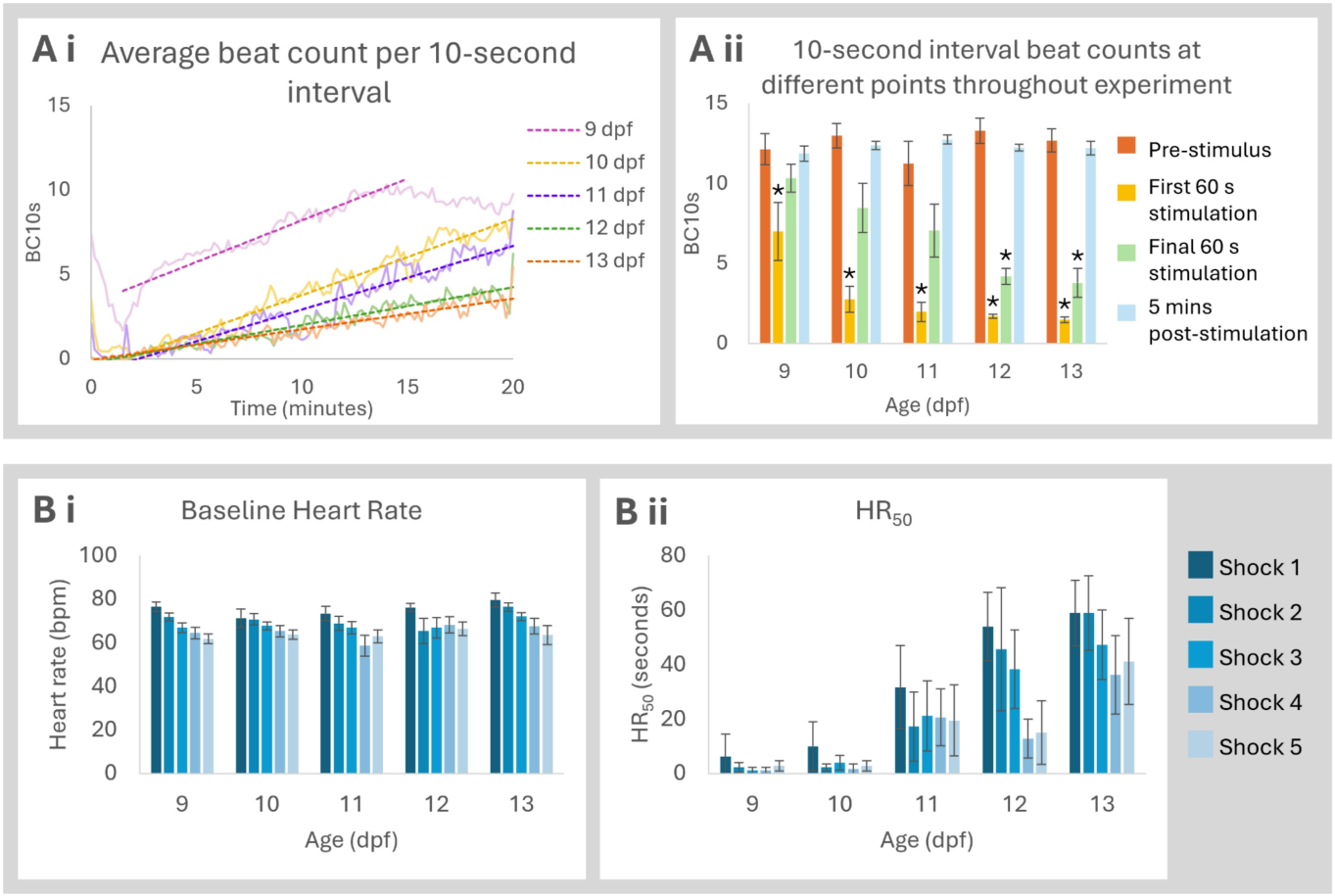

Figure 6

Effect of repeated stimulation on HSPD across development. n=9 embryos per group. (A) Cardiac activity during repeated 10-second stimulation delivered continuously over 20 minutes. **Ai**: Mean beat counts per age group per 10s interval (BC10s) between stimuli across the 20-minute stimulation period. Solid lines indicate the mean for each age. Mean beat counts per 10s interval (BC10s) across the 20-minute stimulation period for each age (9-13 dpf). Solid lines indicate means for each age, dotted lines indicate linear regression models fitted to the post-minimum BC10s recovery period. Goodness of fit (R^2) for each age ranged 0.892-0.961 and RMSE 0.365-0.69. For 9 dpf embryos, the model was only fitted over the first 15 minutes of the post-minimum response period due to non-linear recovery across the full window. **Aii**: Mean BC10s values during four windows throughout the experiment for each age group: pre-stimulus (30 s before stimulation); first 60 s stimulation; final 60 s stimulation mean; 5 mins post stimulation. Error bars show standard error. Asterisks indicate significant differences to baseline BC10s. (B) Response to repeated stimuli delivered at 5-minute intervals across developmental ages. Embryos were recorded for 30 s to obtain baseline heart rate, then stimulation was administered at 30 s. This was repeated five times with the

stimuli delivered at 5 min intervals **Bi** heart rate from the baseline period for each round of stimulation. **Bii** HR_{50}, defined as the time to recover to 50% of the baseline heart rate after each stimulus. Error bars show standard deviation.

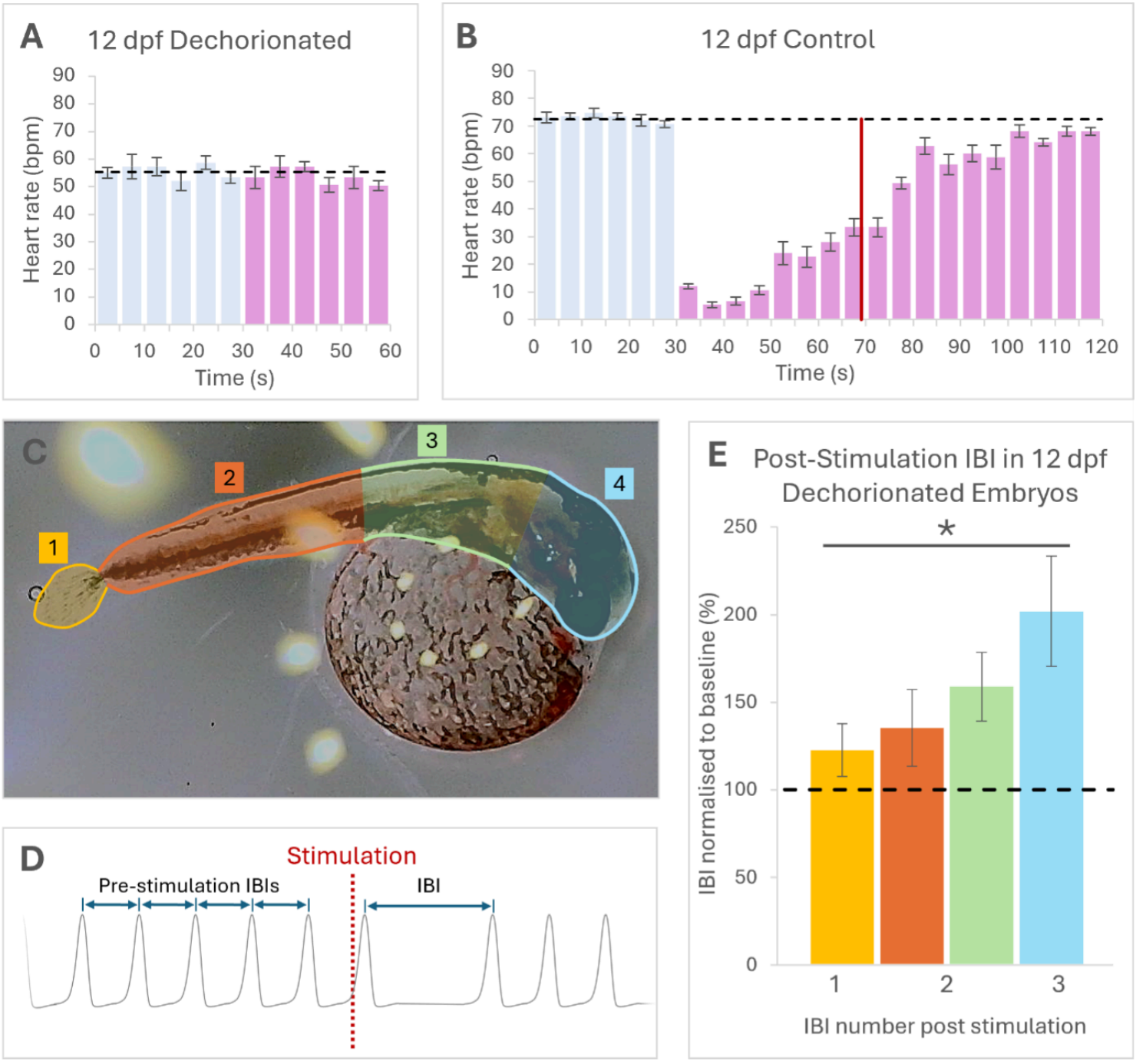

Figure 7

HSPD does not occur in dechorionated 12 dpf embryos from pendulum-tapping assays, although tactile stimulation induces changes in inter-beat intervals (IBIs). For all experiments, *n*=9. (**A, B**) Beat counts over 5-second intervals in embryos before (blue) and after (pink) pendulum-tapping stimulation at 30 seconds. Black dotted lines indicate baseline pre-stimulus heart rate. Error bars in all panels represent standard deviation. **A**. Dechorionated embryos show little change in heart rate following stimulation. **B**. Control (non-

dechorionated) embryos show HSPD behaviour following stimulation. The red vertical line shows time to recover to 50% of baseline heart rate. (**C-E**) Methods and responses to tactile stimulation. **C**. Touch locations used for tactile stimulation. **D**. Schematic showing how IBIs were measured. IBI was defined as time between two beats. For each embryo and touch location, pre-stimulation IBIs were averaged over 30 seconds to define baseline. The first post-stimulation IBI was then measured to compare to baseline. **E**. Post-stimulation IBIs expressed relative to baseline IBI. Colours indicate touch location, as shown in panel **C**. The asterisk and horizontal bar indicate significant differences from baseline, observed for all touch locations. The effect was transient, with subsequent IBIs returning to baseline and therefore not differing significantly differently from baseline. The dashed line indicates baseline (100%).

Supplementary Files

This is a list of supplementary files associated with this preprint. Click to download.

- Supplementary.pdf
- Supplementaryvideo1croppedreducedcompressed.avi
- Supplementaryvideo2.mp4